

A Snow-Ratio Equation and Its Application to Numerical Snowfall Prediction

KUN-YOUNG BYUN, JUN YANG,* AND TAE-YOUNG LEE

Laboratory for Atmospheric Modeling Research, Global Environment Laboratory/Department of Atmospheric Sciences, Yonsei University, Seoul, Korea

(Manuscript received 7 September 2006, in final form 20 June 2007)

ABSTRACT

This study 1) presents a logistic regression equation of the snow ratio (SR) for use in a conversion of numerically predicted precipitation amounts into snowfall depths and 2) examines the quality of snowfall-depth forecasts using the proposed SR equation.

A logistic regression equation of SR has been derived with surface air temperature as the predictor, using observed 3-h snow ratio and surface air temperature. It is obtained for each of several ranges of the precipitation rate to reduce the large variability of SR. The proposed scheme is found to reproduce the observed SRs better than other schemes, according to verification against an independent observation dataset.

Predictions of precipitation and snowfall using the Weather Research and Forecasting (WRF) model and the proposed SR equation have shown some skill for a low threshold [1 mm (6 h)^{-1} and 1 cm (6 h)^{-1} for precipitation and snowfall depth, respectively]: the 10-case mean threat scores (TSs) are 0.47 and 0.43 for precipitation and snowfall forecasts, respectively. For higher thresholds [5 mm (6 h)^{-1} and 5 cm (6 h)^{-1} for precipitation and snowfall depth, respectively], however, TSs for snowfall forecasts tend to be significantly lower than those for the precipitation forecasts. Examination indicates that the poor predictions of relatively heavy snowfall are associated with incorrect prediction(s) of precipitation amount and/or surface air temperature, and the errors of the estimated SRs. The proposed SR equation can be especially useful for snowfall prediction for an area where the spatial variation of precipitation type (e.g., wet or dry snow) is significant.

1. Introduction

At present, snowfall depth forecasting can be viewed as a two-step problem (Roebber et al. 2003). The first step is to make a quantitative precipitation forecast (QPF), and the second step is a conversion of the liquid-equivalent precipitation amount into snowfall depth.

Precipitation forecasting is one of the most challenging goals of numerical weather prediction (NWP). Meanwhile, NWP for winter precipitation can be more reliable than that for summer, since winter precipitation systems are associated mainly with synoptic-scale systems and are less convective than those during the

summer. Olson et al. (1995) found that numerical precipitation forecasts showed increased accuracy in the cold season.

Winter precipitation over the Korean Peninsula is mainly associated with one or more of the following conditions: 1) extratropical cyclones passing over and around the peninsula, 2) moist air flowing toward a mountainous area, and 3) airmass transformation during cold-air outbreaks toward the south (over the warm seas) (Cheong et al. 2006). Thus, NWP should have good potential to forecast winter precipitation over the peninsula, since numerical models tend to produce better predictions for phenomena associated with the conditions mentioned above. However, a complicating feature is that precipitation often occurs in environments with surface air temperatures around 0°C or slightly greater, at which temperatures precipitation can be either snow, rain, or of mixed phase.

Snowfall depth forecasts can be made by converting the liquid-equivalent amount of solid precipitation, predicted by a model with parameterized microphysics, into snowfall depth. To do this, we need to know the

* Current affiliation: NIM, Nanjing University of Information Science and Technology, Nanjing, China.

Corresponding author address: Tae-Young Lee, Dept. of Atmospheric Sciences, Yonsei University, 134 Shinchon-Dong, Seodaemun-Gu, Seoul 120-749, Korea.
E-mail: lty@yonsei.ac.kr

ratio of snowfall depth to liquid-equivalent precipitation amount (hereafter, this ratio will be called the snow ratio, SR).

Changes of precipitation from dry snow in one area to wet snow in a nearby area occur frequently over the Korean Peninsula, and the SR varies significantly in such situations. A snow-ratio formula applicable to such variable situations is desired for accurate numerical snowfall forecasts.

A complex relationship of many factors affects the density of freshly fallen snow (Roebber et al. 2003). As a result, the SR for fresh snow varies greatly depending on the circumstances. For example, Roebber et al. (2003) reported variations from 3 to 100, while this study finds ratios from 0 (i.e., no accumulation) to larger than 50. Various studies have been made to formulate the relation between the snow ratio and meteorological factors (e.g., Kyle and Wesley 1997; Judson and Doesken 2000; Roebber et al. 2003). Roebber et al. (2003) proposed an algorithm in which the snow ratio is determined as one of three classes using a 10-member ensemble of artificial neural networks.

Although no method satisfactorily handles large variations of observed SR, simpler methods are used for operational snowfall forecasts. The National Weather Service (NWS) uses a “new snowfall to estimated meltwater conversion table” as an observing aid in determining the water equivalency of newly fallen snow (National Weather Service 1996). The SR can be obtained from this table for various ranges of surface air temperatures. However, these methods may not provide continuous SR values in an area with significant spatial variation of precipitation composition (i.e., dry or wet snowfalls). A fixed snow ratio of 10 (10-to-1 rule, $SR = 10$) is also used operationally, although several studies have shown that the average SR can differ significantly from 10 (e.g., Judson and Doesken 2000; Roebber et al. 2003; Baxter et al. 2005).

Quantitative snowfall predictions using NWP outputs need an adequate method to convert the liquid-equivalent amount of solid precipitation into snowfall depth in a variety of situations, including snowfall events with significant spatial variations in precipitation type. A relationship that can produce a continuous SR prediction is also desirable for NWP.

The major goals of this study are 1) to obtain a snow-ratio equation and 2) to evaluate the quality of numerical snowfall-depth forecasts using the proposed SR equation and the Weather Research and Forecasting model (WRF; Skamarock et al. 2005). For this study, observed meteorological data are used to derive a nonlinear regression equation of SR. Numerical simulations for 10 snowfall cases over the Korean Peninsula

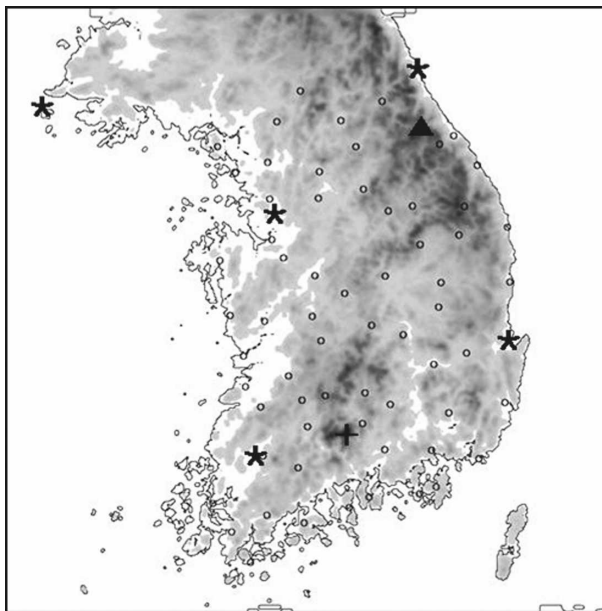


FIG. 1. The topography and locations of the stations for surface (open circles) and upper-air (asterisks) observations. The filled triangles and plus signs indicate the locations of major mountain peaks near the east coast of the midpeninsula and the southern part, respectively. One upper-air station at Jeju Island ($33^{\circ}31'N$, $126^{\circ}32'E$), located to the south of the Korean Peninsula, is not included in this figure.

were used to evaluate the accuracy of snowfall forecasts using the proposed SR equation.

This paper is arranged in the following manner. Section 2 describes the relationships between the observed snow ratio and the meteorological variables and the derivation of a nonlinear (logistic) regression equation of SR. Section 3 includes the descriptions of the experimental design and snowfall events, as well as the evaluation of snowfall predictions for the 10 cases. Conclusions are given in section 4.

2. Determination of snow ratio

A regression equation of SR is obtained here, based on the relationships between the observed snow ratio and other meteorological fields. Both surface and upper-air observations are considered. Data for surface air temperatures higher than $4^{\circ}C$ are not used.

The 3-hourly surface observations are taken from about 70 stations in South Korea (Fig. 1). The 3-hourly fresh snow depth is measured using a snow plate of 50 cm \times 50 cm width. Upper-air observation data are taken from six radiosonde sites (Fig. 1).

The dependence of snow ratio on temperature at various levels is shown in Fig. 2. The temperatures are taken from six radiosonde stations in South Korea for the 22 yr between 1983 and 2004. Upper-air data are

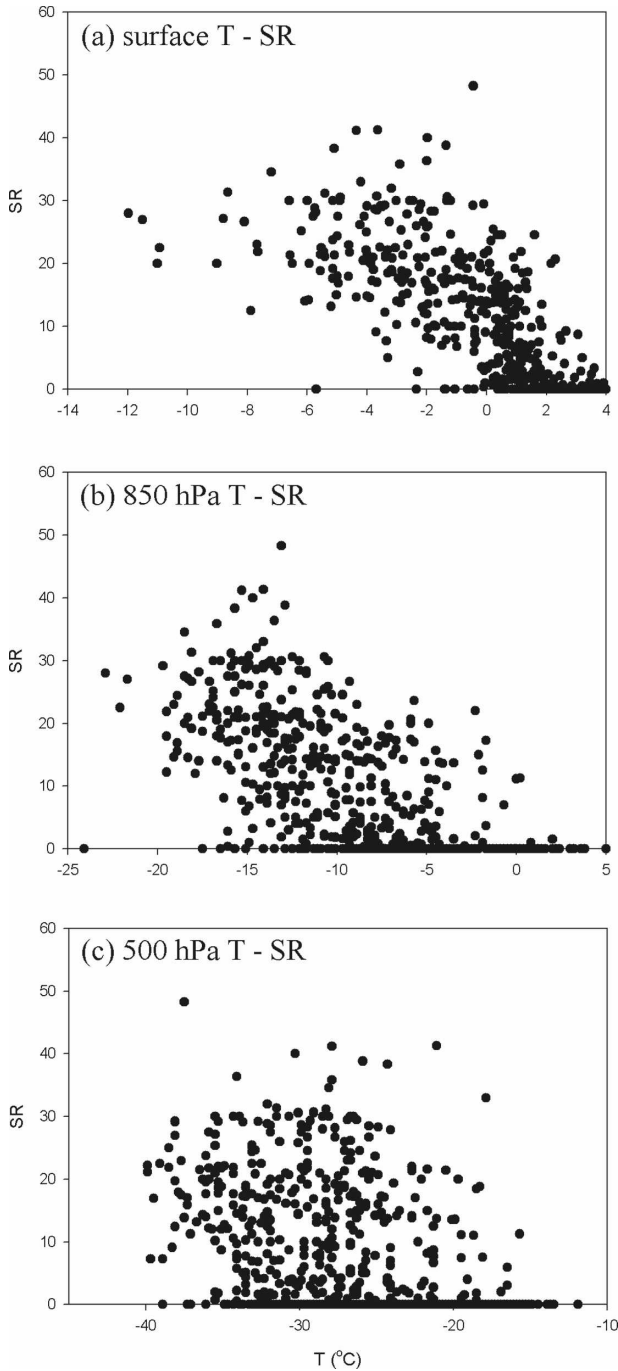


FIG. 2. Observed SR for 6-h precipitation vs temperature at (a) the surface and (b) 850 and (c) 500 hPa.

matched with 6-hourly SRs at the same station except for one, for which a nearby surface station is used. For example, upper-air data for 1200 UTC are matched with the SR for the 6-h period of 0900–1500 UTC. Precipitation rates of less than 1 mm (6 h)^{-1} are not considered in this diagram to avoid the large variations of SR associated with small precipitation amounts.

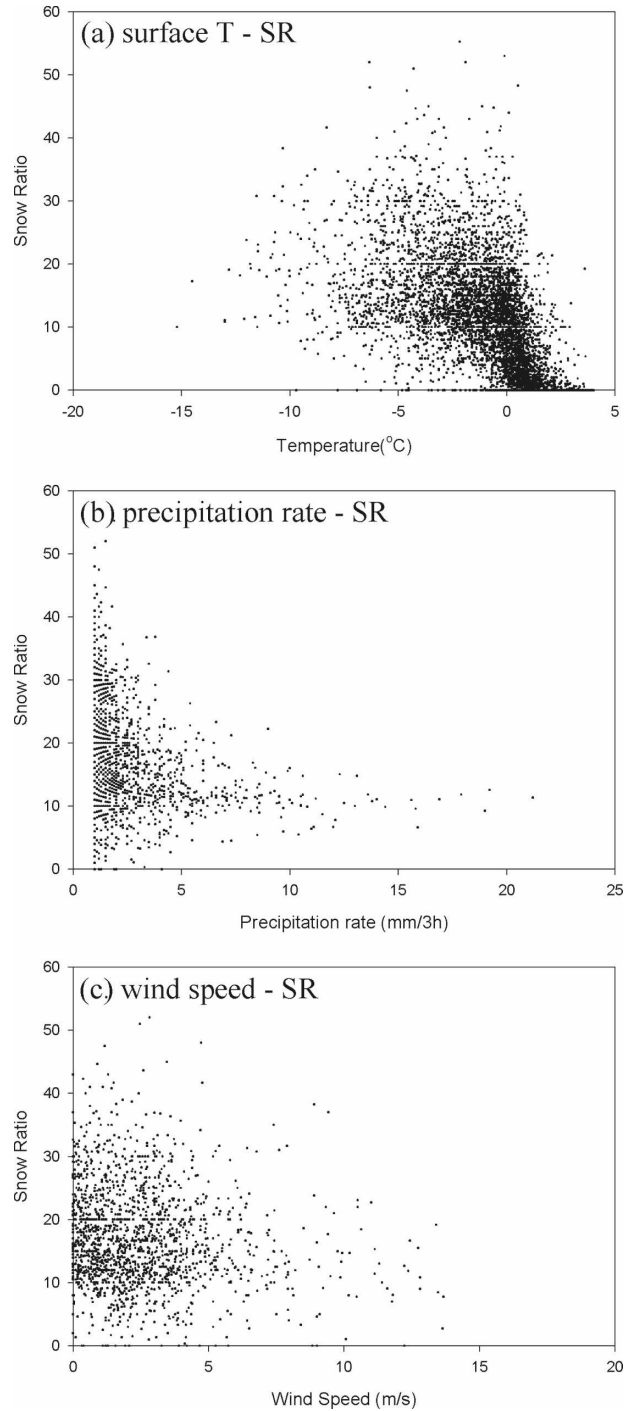


FIG. 3. Scatterplots of observed SR for 3-h precipitation vs surface meteorological fields: (a) surface air temperature, (b) precipitation rate, and (c) wind speed. Precipitation rates of less than 1 mm (3 h)^{-1} are not considered in this diagram to avoid too large variations of SR associated with small precipitation amounts. For (b) and (c), data with surface air temperatures higher than -2°C are also excluded to consider dry snow only.

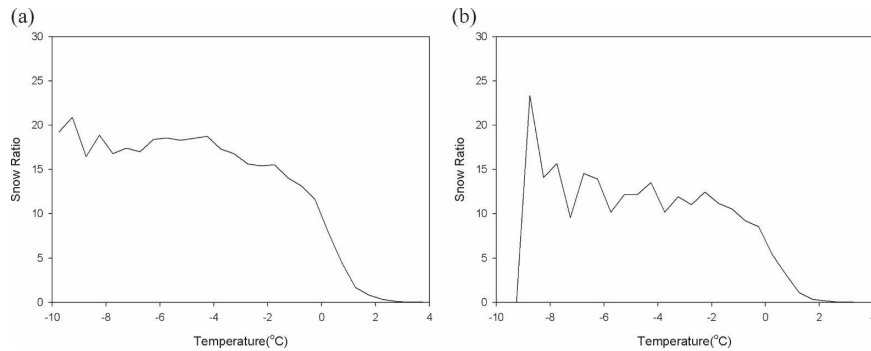


FIG. 4. Smoothed SR (averaged over 0.5°C intervals of surface air temperature) for data with PRs greater than (a) 1 and (b) 5 mm (3 h)^{-1} . Large variations of SR for temperatures lower than -7°C are due to the small amount, or complete lack, of data.

The snow ratio shows a significant dependence on the surface air temperature for temperatures near 0°C and above: The SR decreases rapidly with temperature and becomes close to 0 for temperatures greater than about 1°C . For temperatures lower than 0°C , SR is more scattered and does not show any noticeable dependence on temperature. As height increases, the degree of scatter becomes larger, and small SR values (i.e., smaller than 10) are found throughout the entire temperature range. Note that the upper-level temperatures for the snow episodes are mostly below the freezing point. This is also found at 925 hPa (not shown). These may suggest that, at least for this study, the wetness of the snow is determined mostly by the temperature near the surface. This differs from the findings of Diamond and Lowry (1954), who suggested a stronger correlation of SR with air temperature at 700 hPa. In this study, SR correlates strongly with surface air temperature for the wet snow temperature range, while the correlation with temperature decreases with height.

Scatter diagrams for SR and the surface meteorological variables are shown in Fig. 3. [Precipitation rates of less than 1 mm (3 h)^{-1} are not considered.] Since there are many more surface observation stations than radiosonde stations, the diagram for SR and surface air temperature is shown again in Fig. 3a, but this time using surface observation data for the 8-yr period of 1997–2004. Here, SR is obtained using observed 3-h depths of snow and precipitation, and the surface air temperature is a 3-h average. A strong negative correlation is found again for the wet snow temperature range, while a very large scatter is found for dry snow. Note that a large portion of the data is found in the wet snow range.

To show the effects of the precipitation rate and surface wind speed on the SR of dry snow only, data with surface air temperatures higher than -2°C are also excluded in Figs. 3b and 3c. In this event, the snow ratio shows a significant dependence on precipitation rate

(Fig. 3b), approaching a value near 12 as the precipitation rate increases. The variability of SR becomes larger as the precipitation rate gets smaller. For small precipitation rates, the SR value can be as large as about 50. The large variability of SR for small precipitation rates may be due to many factors, such as meteorological conditions, microphysical structure, observation systems and sites, etc. Surface winds do not seem to show any noticeable relationship with SR (Fig. 3c). Surface relative humidity also does not affect SR significantly (not shown).

According to this study, precipitation rate is the dominant factor for the SR of dry snow, while surface air temperature appears to be the most important predictor for the SR of wet snow. Other surface variables such as wind speed and relative humidity do not show any appreciable relationship with SR.

For dry snow, an average snow ratio (SR_d) as a function of precipitation rate appears to be a more practical approach for an operational snowfall forecast, since no set of predictors seems to fit the wide range of observed SRs. A smoothed SR (averaged over 0.5° intervals of surface air temperature) shows a curve that approaches approximately SR_d for colder temperatures, and zero for above freezing temperatures (Fig. 4). Figure 4 also indicates that SR_d can vary significantly with precipitation rate.

In this study, we have employed a logistic regression analysis using surface air temperature as the predictor to obtain a relationship for SR for a given range of precipitation rates. Logistic regression is employed mainly because SR is assumed to vary between a constant (average) dry snow ratio (SR_d) and 0, and its curve fits the data for the wet snow range well (i.e., for temperature higher than -2°C).

The surface air temperature reflects the temperatures of the ground surface and the air just above the surface, which affects the conditions of the deposited

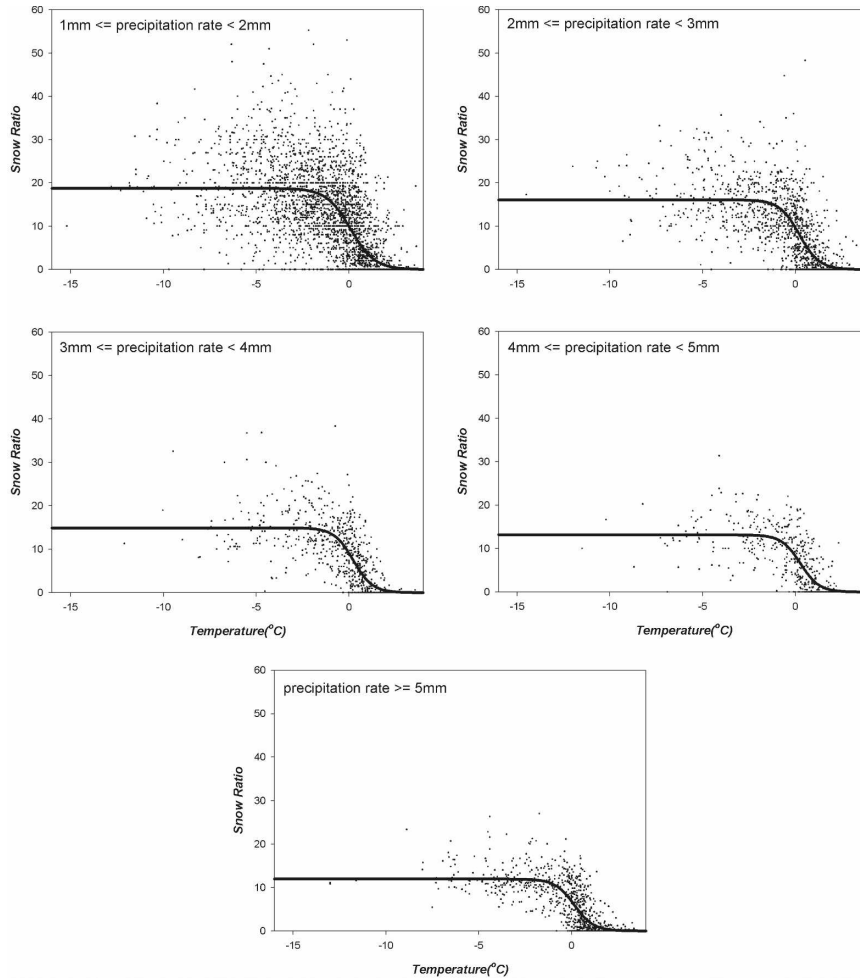


FIG. 5. Observed SR for 3-h precipitation as a function of surface air temperature ($^{\circ}\text{C}$) for each of five ranges of the PR. Curves represent the logistic regression lines obtained for each PR range.

snow over the ground. For this reason, the regression analysis using surface air temperature as the predictor gives a smaller mean square error (MSE) of the estimated SR than do those using temperatures at upper levels (not shown). Multiple logistic regression analysis including other predictors (e.g., temperatures at the 925- and 850-hPa levels) does not decrease the MSE significantly (not shown). Thus, surface air temperature (T) is considered to be the primary predictor, and precipitation rate (PR) is used as the control factor for SR_d .

Since the number of surface observation stations is much larger than that of the radiosonde stations, the final logistic regression analysis has been carried out using surface observation data. A total of 10 512 surface observations (for the 8-yr period of 1997–2004) are used in the derivation of the regression equation. The SR equation is obtained for each of several ranges of PR to reduce the large variability of SR at lower temperatures (Fig. 5):

$$\text{SR} = a / \{1 + \exp[(T - b)/c]\}, \quad (1)$$

$$\begin{aligned} a = 18.8, b = 0.0811, c = 0.6508, & \quad 1 \text{ mm (3 h)}^{-1} \leq \text{PR} < 2 \text{ mm (3 h)}^{-1}, \\ a = 16.1, b = 0.2182, c = 0.5373, & \quad 2 \text{ mm (3 h)}^{-1} \leq \text{PR} < 3 \text{ mm (3 h)}^{-1}, \\ a = 14.9, b = 0.2295, c = 0.5174, & \quad 3 \text{ mm (3 h)}^{-1} \leq \text{PR} < 4 \text{ mm (3 h)}^{-1}, \\ a = 13.2, b = 0.2678, c = 0.5074, & \quad 4 \text{ mm (3 h)}^{-1} \leq \text{PR} < 5 \text{ mm (3 h)}^{-1}, \quad \text{and} \\ a = 11.9, b = 0.1524, c = 0.5174, & \quad \text{PR} \geq 5 \text{ mm (3 h)}^{-1}. \end{aligned}$$

This nonlinear (logistic) regression model for a sigmoidally shaped curve (Ratkowsky 1990) was selected because it gave a better fit, based on the sum of the squared differences, than did other linear and nonlinear (e.g., logistic) models tested in this study. As PR increases, the coefficient a (the average SR for dry snow, SR_d) decreases. According to this study, SR_d for the case of $PR \geq 5 \text{ mm (3 h)}^{-1}$ is 11.9. The SR equation does not seem to change significantly with the length of the data period. It is found that the values of a for the 5-yr period of 1997–2001 are close to those for the 8-yr period of 1997–2004 [cf. Eq. (1)], although the values of b and c show relatively large changes with the length of the data period. The coefficient b represents the temperature at $SR = a/2$, and the coefficient c indicates the degree of slope for the wet snow range. Equation (1) does not have coefficient values for PR smaller than 1 mm (3 h)^{-1} . For the application of Eq. (1) to the numerical snowfall prediction in the next section, the relation for $1 \text{ mm (3 h)}^{-1} \leq PR < 2 \text{ mm (3 h)}^{-1}$ is used for PR smaller than 1 mm (3 h)^{-1} .

The SR relation proposed here is simple enough for operational use and provides continuous SR values. It can be used to predict snowfall for areas where the spatial variation of the precipitation composition (from dry snow in one area to wet snow in a nearby area) is significant, as for the Korean Peninsula.

The present scheme is similar to the scheme used by the National Weather Service (1996) in that surface air temperature is used to determine new snowfall depth. However, in the NWS scheme, SR is obtained from a table of SR values for various surface air temperature ranges. In the NWS table, SR approximate ranges from 10 [for the temperature range of 34° – 28°F (1.1° – -2.2°C)] to 100 [for the range of -21° – -40°F (-29.4° – -40°C)]. In one approximate temperature range [27° – 20°F (-2.78° – -6.67°C)], the precipitation rate also affects the ratio: The SR value varies from 20 at 0.01 in. (0.254 mm) of precipitation to 15 at 0.1 in. (2.54 mm). The main advantage of the present scheme over the NWS table is in that the present scheme includes predictions of the snow ratio for temperatures where wet snow is falling while the NWS scheme does not. This will be demonstrated later (e.g., Fig. 10).

Verification of Eq. (1) is made against an independent dataset (the observations for the period of January 2005–May 2006) that contains 2836 data points. Table 1 shows the correlation coefficient and root-mean-square error (RMSE) of the estimated SR. In Table 1, $SR(T, PR)$ represents the present scheme defined by Eq. (1), while $SR(T)$ represents a scheme that is similar to the present scheme but without considering the precipitation rate [$a = 16.9$, $b = 0.0957$, $c = 0.6001$ in Eq. (1)].

TABLE 1. Correlation coefficient and RMSE between the observed and estimated SRs for snowfall events in January 2005–May 2006. Here, $SR(T, PR)$ represents the proposed scheme [Eq. (1)], where T and PR represent the surface air temperature and precipitation rate, respectively. The $SR(T)$ is the same as in the proposed scheme, except that the PR is not considered [$a = 16.9$, $b = 0.0957$, $c = 0.6001$ in Eq. (1)]. Here, SR_{NWS} represents the NWS scheme. The numbers in parentheses represent the values when the data points with zero SR are excluded.

	$SR(T, PR)$, [Eq. (1)]	$SR(T)$	SR_{NWS}
Correlation coefficient	0.80 (0.55)	0.79 (0.52)	0.71 (0.39)
RMSE	5.20 (6.70)	5.28 (6.81)	6.08 (7.49)

Table 1 also includes the results for the NWS scheme (SR_{NWS}). The correlation of estimated SRs with the observations is good, influenced no doubt by the large number of data points with a zero snow ratio. The snow ratio from the present scheme shows the highest correlation with observations and the smallest RMSE. When the zero points (i.e., data points with zero SR) are excluded, the correlation coefficient becomes significantly smaller as shown in Table 1. However, the coefficient of 0.55 for the present scheme is still a significant value, considering that the correlation is poor for the dry snow range. In other words, good correlation is found for the wet snow range. Regarding the regression analysis, the zero points are necessary since the zero points are a part of the dataset. (Note that data for surface air temperatures higher than 4°C are not used in this study.) The regression equation, derived without the zero points, produces SR values that do not approach zero quickly enough as the surface air temperature increases above the freezing point (not shown). As a result, significant snowfall can be predicted for surface air temperatures well above 0°C (e.g., over 3°C).

The effect of including the precipitation rate, as in Eq. (1), reduces the RMSE by just 0.08. This relatively small improvement may be due to the fact that most data points have small precipitation rates, and only a small number of data points have large rates. When we consider a heavy snowfall event [e.g., an event with a precipitation rate greater than 5 mm (3 h)^{-1}], the reduction of the RMSE should be larger. Thus, SR_d as a function of precipitation rate can be more useful for heavier snowfall events.

3. Numerical snowfall prediction

a. Model and experimental design

The Advanced Research WRF model (ARW, version 2.0.3; Skamarock et al. 2005) is used for this study.

TABLE 2. Snowfall events considered for our numerical snowfall prediction experiment.

Case	Duration of precipitation event (h)	Duration of numerical integration (h)	Type of snowfall event
1	2100 UTC 14 Feb–1800 UTC 15 Feb 2001 (21)	1200 UTC 14 Feb–0000 UTC 16 Feb 2001 (36)	II
2	1200 UTC 19 Jan–0300 UTC 20 Jan 2001 (15)	0000 UTC 19 Jan–1200 UTC 20 Jan 2001 (36)	III
3	1200 UTC 6 Jan–0000 UTC 8 Jan 2001 (36)	0000 UTC 6 Jan–0000 UTC 8 Jan 2001 (48)	V
4	1200 UTC 10 Dec–0600 UTC 11 Dec 1997 (18)	0000 UTC 10 Dec–1200 UTC 11 Dec 1997 (36)	II
5	1800 UTC 4 Jan–0600 UTC 6 Jan 1997 (36)	0600 UTC 4 Jan–0600 UTC 6 Jan 1997 (48)	III
6	2100 UTC 12 Jan–0300 UTC 14 Jan 1992 (30)	1200 UTC 12 Jan–1200 UTC 14 Jan 1992 (48)	IV
7	0300 UTC 3 Jan–2100 UTC 3 Jan 1991 (18)	1200 UTC 2 Jan–0000 UTC 4 Jan 1991 (36)	I
8	0600 UTC 29 Jan–1200 UTC 01 Feb 1990 (78)	1800 UTC 28 Jan–1800 UTC 31 Jan 1990 (72)	V
9	2100 UTC 17 Jan–0900 UTC 20 Jan 1989 (60)	0000 UTC 18 Jan–1200 UTC 20 Jan 1989 (60)	III
10	1500 UTC 23 Dec–0900 UTC 24 Dec 1983 (18)	0000 UTC 23 Dec–1200 UTC 24 Dec 1983 (36)	I

The model physics used in the prediction experiments include the WRF single-moment five-class (WSM5) microphysics scheme, a five-layer soil model for ground temperature (Chen and Dudhia 2000), the Kain–Fritsch cumulus scheme (Kain and Fritsch 1993), and an Medium-Range Forecast model (MRF) PBL scheme (Hong and Pan 1996). The radiation parameterization is modeled using rapid radiative transfer model (RRTM) longwave radiation (Mlawer et al. 1997) and a simple fifth-generation Pennsylvania State University–National Center for Atmospheric Research Mesoscale Model (MM5) shortwave scheme (Dudhia 1989).

Prediction experiments are carried out for the 10 cases listed in Table 2. Experiments have been carried out with 30- and 10-km (nested) grids for the domains shown in Fig. 6. Numerical integrations start 9–15 h ahead of the time of initial precipitation in each case except for case 9. In case 9, the observed precipitation is already occurring before the initial time of the numerical integration. However, major snowfall occurs 3 h after the initial time. Initial and lateral boundary conditions for the 30-km domain are prepared using 6-hourly National Centers for Environmental Prediction (NCEP)–NCAR global reanalysis pressure level ($2.5^\circ \times 2.5^\circ$) data and T62 Gaussian (192×94) NCEP–NCAR global reanalysis surface flux data. The 3-hourly snowfall depth is calculated by multiplying the 3-h total (convective + explicit) precipitation amount by the SR, as defined by Eq. (1). The 3-h-average surface air temperature is used to obtain SR. In the verification of the model results, the predicted value at an observation station is obtained by a linear interpolation from the values at model grids.

b. Snowfall events

Ten snowfall events have been selected for this study, after a review of all of the snowfall events over the Korean Peninsula from 1983 to 2001, in which more

than 20 cm of daily fresh snowfall is found at least at one station (Table 2). The selection is made in a manner such that one or more cases is included for each of the major snowfall types found over the Korean Peninsula. Cheong et al. (2006) have classified the snowfall events over the peninsula into five types based on the mechanism of snowfall development:

- type I—snowfalls associated with airmass transformation during cold-air outbreaks from the northeastern Asian continent toward the south (over the warm sea surfaces),
- type II—snowfalls associated with extratropical cyclones passing over the peninsula,
- type III—snowfalls associated with extratropical cyclones passing over the sea to the south of the peninsula,
- type IV—snowfalls associated with a mesoscale trough over the peninsula with the Siberian high expanding toward the northeast and the southwest of the peninsula (Lee and Park 1996), and
- type V—snowfalls associated with the combined synoptic situations of types III and IV or similar situations to that for type IV, except that an extratropical cyclone to the south of the peninsula induces a trough over the peninsula.

Moisture transport toward the peninsula and terrain effects are important for types III and V, while terrain effects and airmass transformation are important for snowfalls of type IV. The snowfall cases listed in Table 2 are classified according to these typical situations.

c. Results

Table 3 shows a comparison between the observed and predicted depths of precipitation and snowfall for the 10 cases. The depths are the averages over the stations in South Korea. The precipitation and snow depths are accumulated over the entire period of precipitation.

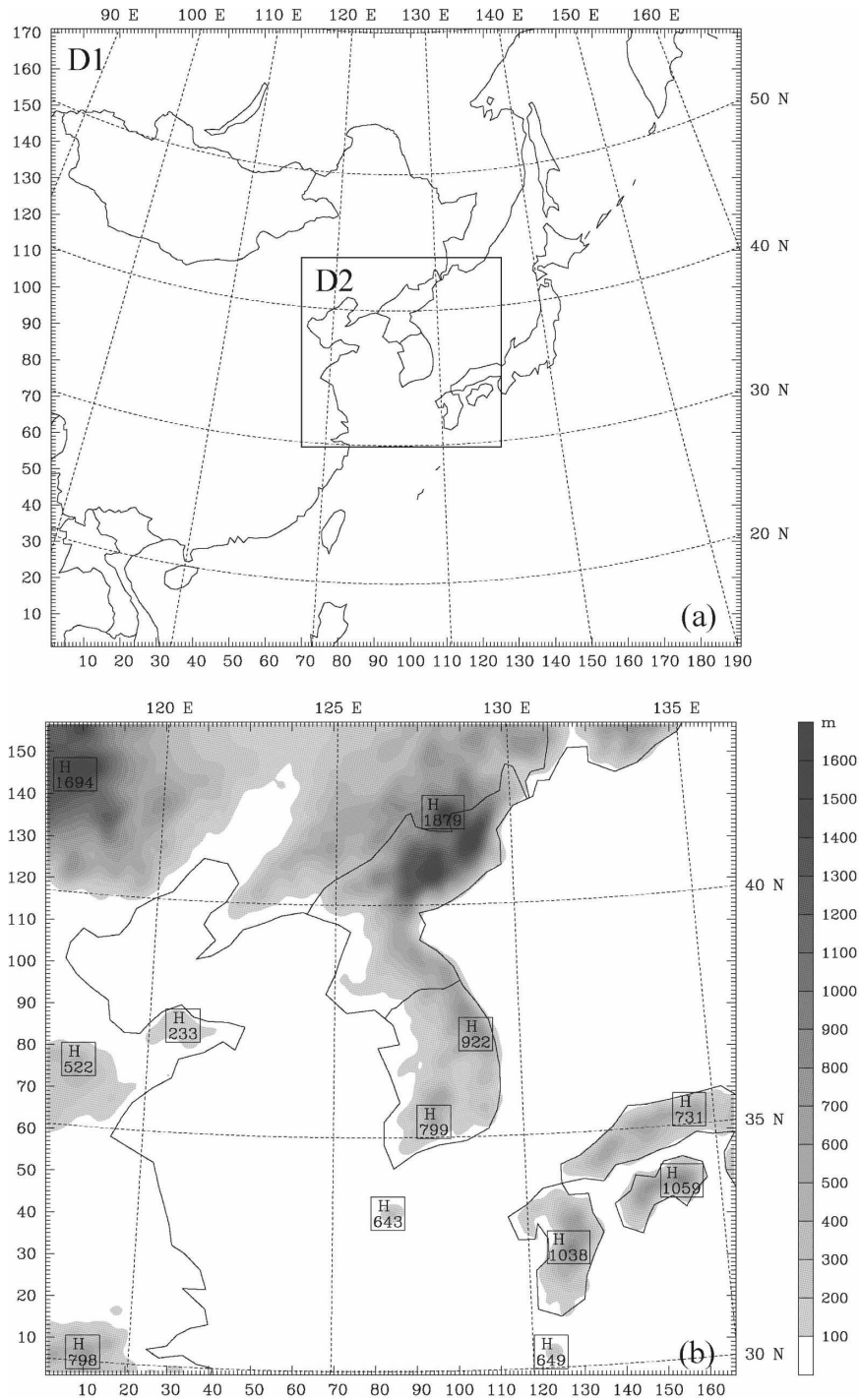


FIG. 6. (a) Computational domains and (b) model topography in domain 2. The grid sizes for domain 1 (D1) and domain 2 (D2) are 30 and 10 km, respectively.

In general, predicted amounts of precipitation are comparable to the observed values, although some cases show significant differences between the two. The correlation between the predicted and observed precipitation is generally fair, with the correlation coefficient

being greater than 0.55 in seven of the cases. However, the model tends to overpredict the precipitation amount. Five cases show a significant overprediction of more than 50%, while two cases show a significant underprediction. But, when we consider that very large

TABLE 3. Precipitation and snowfall depths from observations and predictions, averaged over the stations in South Korea (excluding island stations), and their relative errors (REs) and the coefficient of correlation (r) between the observations and predictions. The RE value for each case is a bulk relative error obtained using case mean precipitation amounts or snow depths before they are rounded off to the first decimal place. The mean values in parentheses are the values computed by combining the data over all of the cases and treating them as a single case.

Case	Precipitation (mm)				Snowfall depth (cm)			
	Observation	Prediction	RE (%)	r	Observation	Prediction	RE (%)	r
1	5.9	9.3	56.8	0.59	5.2	5.4	3.4	0.53
2	8.7	8.3	-4.5	0.76	3.4	1.2	-66.3	0.32
3	27.5	31.2	13.5	0.75	10.7	8.8	-17.6	0.58
4	2.8	5.6	103.7	0.66	4.9	7.0	43.7	0.63
5	6.7	23.3	249.6	0.37	9.3	17.0	83.0	0.37
6	3.1	4.0	30.8	0.89	2.7	3.5	31.9	0.77
7	1.0	2.9	186.3	0.56	2.0	3.8	89.4	0.51
8	21.4	14.1	-34.0	0.62	22.4	11.8	-47.4	0.81
9	28.0	16.5	-41.1	0.49	1.9	1.3	-27.2	0.85
10	1.2	3.1	169.8	0.51	2.8	5.2	83.1	0.60
Mean	10.6	11.9	73.1 (11.3)	0.62 (0.63)	6.5	6.5	17.6 (-0.4)	0.60 (0.59)

REs are found for cases with relatively small observed precipitation (e.g., cases 7 and 10), the amount of overprediction is not as great as is indicated by the 10-case average RE value. Actually, the 10-case average precipitation amounts from the predictions and the observations differ from each other by 1.3 mm. And the mean RE, computed by combining the data over all of the cases and treating it as a single case, is just 11.3%.

In general, the predicted snow depths also match the observations well, although a tendency for overprediction is found here as well. However, the degree of overprediction is not as significant as that for precipitation forecasts. Furthermore, when we exclude the cases with small precipitation amounts (e.g., cases 7 and 10), no noticeable tendency for overprediction can be found. This may indicate that the present snow depth forecasts actually have a tendency toward underprediction, when

we consider the significant overprediction of precipitation.

Table 4 shows the forecasting skill for the 6-h precipitation and snow depth. The threat scores (TSs) for low thresholds of precipitation and snow depths are fairly high. The 10-case mean TS values are 0.47 and 0.43 for the precipitation and snowfall forecasts, respectively. For higher thresholds, TSs for snowfall forecasts tend to be significantly lower than those for precipitation forecasts. They are smaller than 0.2 in five cases, with a zero score for two of the cases (cases 2 and 7). Relatively high TSs are found for cases in which terrain-induced snowfalls are significant (e.g., cases 1, 6, and 8). According to the bias score (BS), a snowfall depth greater than 5 cm is not predicted at all for case 2, while its location is predicted incorrectly in case 7. The mean TSs, computed by combining the data over

TABLE 4. Skill scores for predictions of 6-h precipitation and snowfall depths. The mean values in parentheses are the values computed by combining the data over all of the cases and treating them as a single case.

Case	Threat score				Bias score			
	Precipitation threshold		Snow depth threshold		Precipitation threshold		Snow depth threshold	
	1 mm	5 mm	1 cm	5 cm	1 mm	5 mm	1 cm	5 cm
1	0.57	0.39	0.42	0.27	1.57	1.50	1.38	0.96
2	0.63	0.62	0.20	0.00	1.27	0.98	0.59	0.00
3	0.81	0.69	0.52	0.20	1.16	1.16	1.00	0.65
4	0.49	0.08	0.60	0.15	1.82	3.33	1.41	1.62
5	0.34	0.18	0.36	0.15	2.19	3.82	1.56	1.63
6	0.35	0.47	0.49	0.29	1.62	1.44	1.48	1.25
7	0.30	0.00	0.38	0.00	2.50	0.00	1.59	1.60
8	0.57	0.15	0.50	0.28	0.77	0.44	0.73	0.48
9	0.35	0.28	0.32	0.22	0.43	0.65	0.79	0.38
10	0.24	0.00	0.46	0.16	3.48	1.00	1.78	1.75
Mean	0.47 (0.49)	0.29 (0.38)	0.43 (0.45)	0.17 (0.20)	1.68 (1.09)	1.43 (1.05)	1.23 (1.14)	1.03 (0.85)

all of the cases and treating it as a single case, are higher than the 10-case mean TSs (simple average of the column). The opposite is true for the mean BSs.

As shown in Table 2, the duration of the numerical integration varies by case from 36 to 72 h. It is possible that the length of the integration period affects the accuracy of the prediction. However, the skill scores in Table 4 do not clearly show their dependence on integration length. In case 9, which has a relatively longer integration period, the quality of the prediction is significantly poorer in the later part of the integration period than that in the earlier part. However, such a tendency is not clear in case 8, which has the longest integration period. The effects of integration length may be obscured by other factors that can affect the prediction accuracy, such as the quality of the initial conditions, physics of precipitation development, etc.

In the results shown in Table 4, cases 2 and 3 show significant degradation of forecasting skill for snowfall compared to those for precipitation, while the opposite is true for cases 8 and 10. Correlation coefficients in Table 3 also show similar differences in performance between precipitation and snowfall predictions for those cases. Here, we examine these cases in more detail. Figure 7 shows the spatial distribution of the predicted precipitation and snow depths as compared with the observations. In case 2 (Fig. 7, top), for which the TS for the snowfall forecast is 0 for a higher threshold [≥ 5 cm (3 h) $^{-1}$], precipitation is found throughout South Korea and its amount increases toward the south. Precipitation over the southern part appears to be mostly in the form of rain. The predicted precipitation agrees well with the observations, although the relatively large amount in the western part of South Korea is not predicted. Observed snowfalls are limited to the mountainous area (marked by plus signs) and to its north, where the maximum snow depth is found. Snowfall prediction shows limited success. The predicted snow area agrees with the observations to some extent. However, the predicted snow depths are much smaller than are observed, especially over mountainous areas. This underprediction of snow depth appears to be due to 1) an underpredicted precipitation amount around the mountainous areas (Fig. 7b) and 2) a small estimated snow ratio (Fig. 8b, top). The snow ratio shown in Fig. 8 is obtained using the accumulated depths of the snow and precipitation for the snowfall period of each case. The estimated SRs over the mountain area and to its north are much smaller than 10 (Fig. 8b), while the observed values are greater than 10 (Fig. 8a). This underestimation seems to be due primarily to the relatively higher predicted temperatures than the

observations (Fig. 9, top). This will be described in detail later.

In case 3, for which the TSs for snowfall forecasts at a 5-cm threshold are significantly lower than those for the precipitation forecasts at a 5-mm threshold, the model has reproduced the observed precipitation fairly well (Figs. 7e and 7f). Again, snowfall prediction shows limited success (Figs. 7g and 7h). The model has reproduced the observed maximum snow depth over the mountainous area near the east coast in the midpeninsula, and the predicted snowfall area agrees fairly well with the observations. However, significant portions of the area with observed snow depths greater than 5 cm are not predicted properly. Also, the predicted snow depth is too large for the east coast area on the right side of the maximum snow depth, where the observed precipitation is mostly rain. As shown in Fig. 8f, the estimated SRs are significantly smaller than the observed values in much of the snowfall area, while the opposite is true in the east coast area where the observed SRs are less than 1. These features will be explained later by examining the predicted temperature.

In case 8, the threat score for snow depth forecasts for the higher threshold is larger than that for precipitation forecasts (Table 4). In this case, significant precipitation is observed throughout South Korea, with a maximum amount of greater than 130 mm over the mountainous area in the midpeninsula (Fig. 7i). The model has predicted precipitation throughout South Korea, with a maximum over the mountainous area in the midpeninsula (Fig. 7j). However, the simulated amounts are significantly smaller than the observations, especially over the western part of the country and the mountainous areas. The distribution of the observed snow depth resembles that of the observed precipitation, except that the observed precipitation over the southeast coast is mostly rain. The model has reproduced well the general pattern of observed snow depth. As for precipitation, the predicted snow depths are significantly smaller than the observations. In this case, the estimated SRs are well matched with the observed values (Figs. 8i and 8j). Thus, the underprediction of snow depth in this case seems to be mainly due to the underprediction of the precipitation amount.

A comparison between the observed and predicted surface air temperatures is shown in Fig. 9 to explain the cause of the under- or overpredictions of snowfall in cases 2, 3, and 8. The values shown in the figure are for the case-mean temperatures. The predicted temperature compares favorably with the observations in general, although the pattern of the difference [prediction (PRE) - observation (OBS)] varies by case. In case 2, the predicted temperatures are higher than the obser-

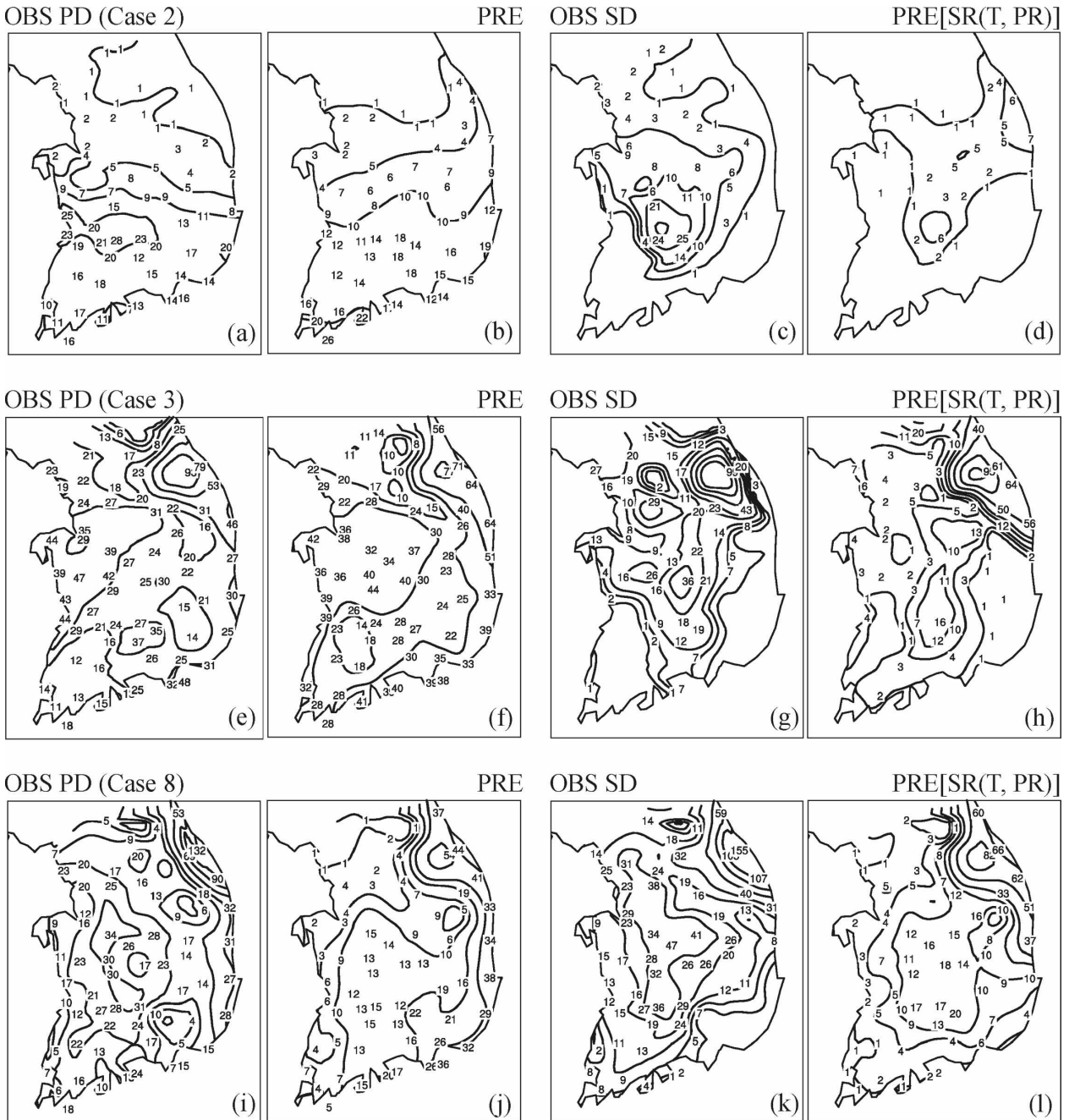


FIG. 7. Spatial distribution of the observed (OBS) and predicted (PRE) depths of the precipitation (PD) and snowfall (SD) for cases (top) 2, (middle) 3, and (bottom) 8. The predictions are from a 10-km grid model. Contours are for 1, 5, 10, 20, 30, 50, 70, and 100 mm (cm) and the two left (right) panels are for precipitation (snow depth).

vations in most of the area except along the east coast, where significant underpredictions are found (Fig. 9, top). Along the east coast of the midpeninsula, the predicted temperatures are near or below freezing, while the observations are in the range of 2°–4°C. Case 3 shows a pattern of differences similar to that in case 2. However, the areas of under- and overprediction are

comparable to each other (Fig. 9, middle). For case 8, the predicted temperatures are lower than the observations in most of the area, unlike in the other two cases (Fig. 9, bottom). A common feature shown in Fig. 9 is that, in the mountainous area of the midpeninsula (marked by a triangle), the predicted mean temperature is higher than the observation.

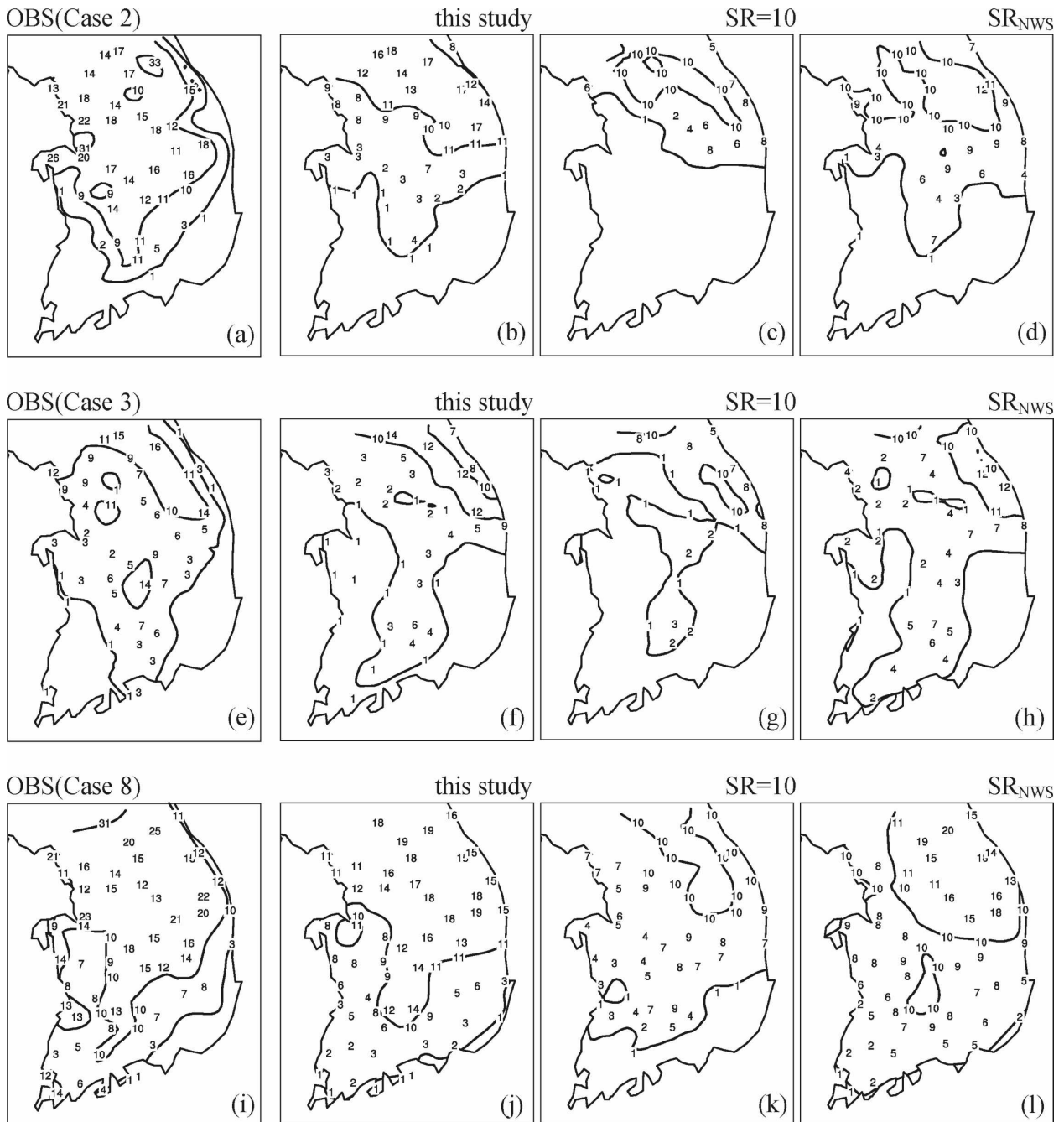


FIG. 8. (a), (e), (i) Observed and predicted SRs from experiments using (b), (f), (j) the present SR equation; (c), (g), (k) a fixed ratio (SR = 10); and (d), (h), (l) the NWS scheme for cases (top) 2, (middle) 3, and (bottom) 8. Contour values are 1, 10, 30, and 50.

One reason for the over- and underpredictions of the surface air temperatures found in Fig. 9 may be the inadequate representation of steep terrain by the 10-km grid model. Steep terrain exists immediately to the west of the eastern coastline of the midpeninsula (Fig. 1). The height of the east coast in the smoothed model terrain is about 290 m higher than the real height, while

the mountaintop height is about 59 m lower. This averaged but inaccurate model terrain may be a reason for the lower and higher predicted temperatures over the east coast and the mountainous areas, respectively.

Table 5 shows the 10-case averages of the correlation coefficient and the threat and bias scores for forecasts of 6-h snow depth. Forecasts using the NWS table show

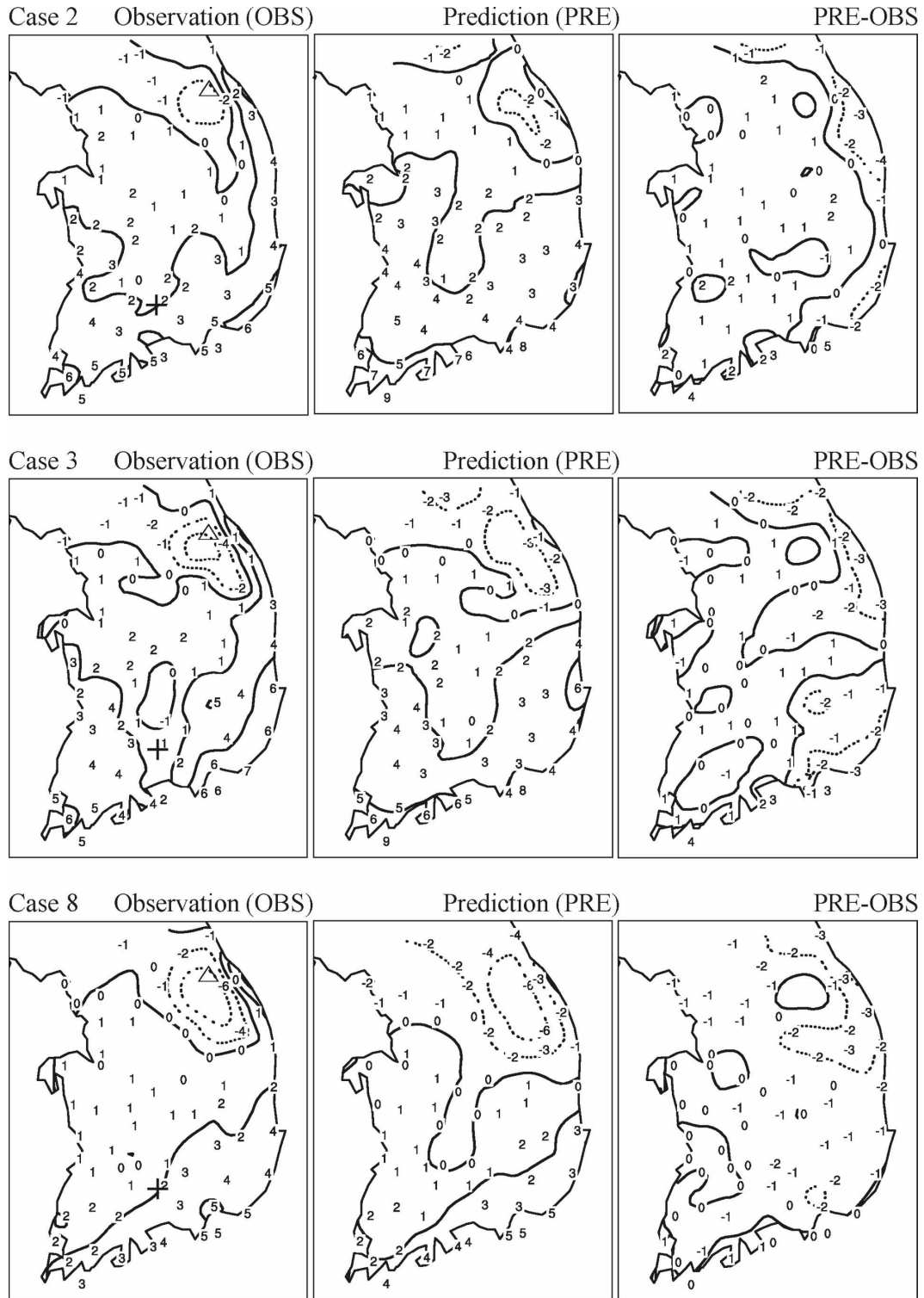


FIG. 9. (left) Observed and (middle) predicted case-mean temperatures and (right) their difference for case (top) 2, (middle) 3, and (bottom) case 8. Contour values are -5° , -2° , 0° , 2° , and 5°C .

TABLE 5. Ten-case mean skill of snowfall predictions: correlation coefficient (r) between predicted and observed snowfall depths, TS and BS of snowfall predictions using the present SR scheme [SR(T , PR), Eq. (1)], a fixed ratio of 10 ($SR = 10$), and the NWS scheme (SR_{NWS}). The numbers in parentheses are the values computed by combining the data over all of the cases and treating them as a single case.

	SR(T , PR): Eq. (1)	SR = 10	SR _{NWS}
r	0.60 (0.59)	0.54 (0.52)	0.58 (0.57)
TS(1cm)*	0.43 (0.45)	0.35 (0.36)	0.42 (0.44)
BS(1cm)*	1.23 (1.14)	0.84 (0.79)	1.21 (1.13)
TS(5cm)*	0.17 (0.20)	0.12 (0.13)	0.19 (0.21)
BS(5cm)*	1.03 (0.85)	0.41 (0.39)	0.99 (0.86)

* The numbers in the parentheses represent the threshold values of the snowfall depth.

skill that is close to that of the present scheme. Forecasts with the 10-to-1 rule show relatively poor skill. The small difference in the forecast skill between the present and the NWS schemes seems to be partly due to the fact that both schemes consider surface air temperature as the predictor. However, given that the present scheme reproduces the observed SR better than does the NWS scheme (see Table 1), other causes (e.g., accuracy of predicted precipitation and surface air temperature) may also be important reasons for such small differences.

An important advantage of the present formulation over the NWS scheme can be found when we consider a short period of time (e.g., 3 h) with significant spatial variation of temperature. Figure 10 shows the observed and estimated SRs for the 3-h period of 0900–1200 UTC 30 January 1990. The observation shows a gradual decrease of SR from 10 to 0 in the southern area. Es-

timated SRs using the present scheme agree better with the observations than those of the NWS scheme. Snow ratios from the NWS scheme show abrupt changes from 10 to 0 across the boundary of the snow area.

4. Conclusions

This study has 1) presented a logistic regression equation of snow ratio (SR) for use in converting numerically predicted precipitation amounts into snowfall depths and 2) examined the quality of snowfall-depth forecasts using the proposed SR equation.

According to our results, precipitation rate is the dominant factor for the SR of dry snow, while surface air temperature is found to be the most important predictor for the SR of wet snow. For dry snow, the average snow ratio (SR_d) as a function of precipitation rate appears to be a more practical approach for operational snowfall forecasts, since no predictors can fit the wide range of observed snow ratios in a satisfactory manner.

In this study, a logistic regression equation of the SR has been obtained with surface air temperature as the predictor, using the observed 3-h snow ratio and surface air temperature. The regression equation is obtained for each of several ranges of precipitation rates to reduce the large variability of SR. Here, the SR equation is for the 3-h snowfall depth. Logistic regression is employed mainly because the SR is assumed to vary between a constant (average) dry snow ratio (SR_d) and zero, and its curve fits the data well for the wet snow range (i.e., for temperatures higher than -2°C). The proposed scheme is found to reproduce the observed SRs better than other schemes do, according to verification against an independent observation dataset.

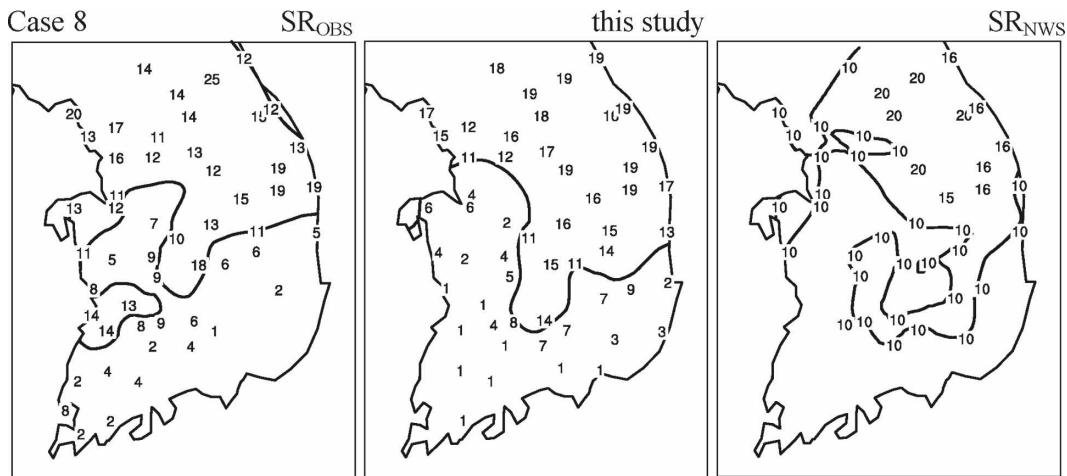


FIG. 10. (left) Observed SR and (right) SRs estimated by the (middle) present and (right) NWS schemes for 0900–1200 UTC 30 Jan 1990 in case 8. Only one contour is shown for the value 10.

The WRF model has shown some skill in predicting precipitation and snowfall for low thresholds [1 mm (6 h)^{-1} and 1 cm (6 h)^{-1} for precipitation and snowfall depth, respectively]. The 10-case mean threat scores (TSs) are 0.47 and 0.43 for precipitation and snowfall forecasts, respectively. For higher thresholds [5 mm (6 h)^{-1} and 5 cm (6 h)^{-1} for precipitation and snowfall depth, respectively], however, TSs for snowfall forecasts tend to be significantly lower than those for precipitation forecasts. They are lower than 0.2 in five cases, with a zero score for two of the cases. Examination indicates that the poor predictions of relatively heavy snowfall are associated with incorrect prediction(s) of precipitation amounts and/or surface air temperatures, compounded by the errors of the estimated SRs.

The SR equation proposed here is simple enough for use in operational numerical forecasts and provides continuous SR values. It is found to produce realistic values of SR for the cases considered here, when the prediction of the surface air temperature is realistic. This method can be useful for snowfall prediction for an area where the surface air temperature shows significant spatial variation around the freezing point, and precipitation varies from dry snow in one area to wet snow in a nearby area, as can be the case for the Korean Peninsula.

Acknowledgments. This work was supported by the Korea Foundation for International Cooperation of Science and Technology (KICOS) through a grant provided by the Korean Ministry of Science and Technology (MOST) in 2007 (M60602000007-06E0200-00700).

REFERENCES

- Baxter, M. A., C. E. Graves, and J. T. Moore, 2005: A climatology of snow-to-liquid ratio for the contiguous United States. *Wea. Forecasting*, **20**, 729–744.
- Chen, S.-H., and J. Dudhia, 2000: Annual report: WRF physics. Air Force Weather Agency, 38 pp.
- Cheong, S.-H., K.-Y. Byun, and T.-Y. Lee, 2006: Classification of snowfalls over the Korean Peninsula based on developing mechanism (in Korean). *Atmosphere*, **16**, 33–48.
- Diamond, M., and W. P. Lowry, 1954: Correlation of density of new snow with 700-millibar temperature. *J. Atmos. Sci.*, **11**, 512–513.
- Dudhia, J., 1989: Numerical study of convection observed during the Winter Monsoon Experiment using a mesoscale two-dimensional model. *J. Atmos. Sci.*, **46**, 3077–3107.
- Hong, S.-Y., and H.-L. Pan, 1996: Nonlocal boundary layer vertical diffusion in a medium-range forecast model. *Mon. Wea. Rev.*, **124**, 2322–2339.
- Judson, A., and N. Doesken, 2000: Density of freshly fallen snow in the central Rocky Mountains. *Bull. Amer. Meteor. Soc.*, **81**, 1577–1587.
- Kain, J. S., and J. M. Fritsch, 1993: Convective parameterization for mesoscale models: The Kain–Fritsch scheme. *The Representation of Cumulus Convection in Mesoscale Models*, Meteor. Monogr., No. 46, Amer. Meteor. Soc., 165–170.
- Kyle, J. P., and D. A. Wesley, 1997: New conversion table for snowfall to estimated meltwater: Is it appropriate in the High Plains? NWS Central Region Applied Research Paper 18-04, NOAA/NWS, Cheyenne, WY, 4 pp. [Available online at <http://www.crh.noaa.gov/crh/?n=arp18-04>.]
- Lee, T.-Y., and Y.-Y. Park, 1996: Formation of a mesoscale trough over the Korean Peninsula during an excursion of the Siberian high. *J. Meteor. Soc. Japan*, **74**, 299–323.
- Mlawer, E. J., S. J. Taubman, P. D. Brown, M. J. Iacono, and S. A. Clough, 1997: Radiative transfer for inhomogeneous atmosphere: RRTM, a validated correlated-k model for the longwave. *J. Geophys. Res.*, **102** (D14), 16 663–16 682.
- National Weather Service, 1996: Surface weather observations and reports. Part IV: Supplemental observations. National Weather Service Observing Handbook 7, Silver Spring, MD, 57 pp.
- Olson, D. A., N. W. Junker, and B. Korty, 1995: Evaluation of 33 years of quantitative precipitation forecasting at NMC. *Wea. Forecasting*, **10**, 498–511.
- Ratkowsky, D. A., 1990: *Handbook of Nonlinear Regression Models*. Marcel Dekker, 241 pp.
- Roebber, P. J., S. L. Bruening, D. M. Schultz, and J. V. Cortinas Jr., 2003: Improving snowfall forecasting by diagnosing snow density. *Wea. Forecasting*, **18**, 264–287.
- Skamarock, W. C., J. B. Klemp, J. Dudhia, D. O. Gill, D. M. Barker, W. Wang, and J. G. Powers, 2005: A description of the Advanced Research WRF Version 2. NCAR Tech Note NCAR/TN-468+STR, 88 pp.